Families of Superhard Crystalline Carbon Allotropes Constructed via Cold Compression of Graphite and Nanotubes

Haiyang Niu, Xing-Qiu Chen, Shibing Wang, Dianzhong Li, Wendy L. Mao, and Yiyi Li

Phys. Rev. Lett. **108**, 135501 — Published 28 March 2012

DOI: 10.1103/PhysRevLett.108.135501

Families of superhard crystalline carbon allotropes induced via cold-compressed graphite and nanotubes

Haiyang Niu[1], Xing-Qiu Chen[1,*] Shibing Wang[2], Dianzhong Li[1], Wendy L Mao[2,3], Yiyi Li[1]
[1] *Shenyang National Laboratory for Materials Science, Institute of Metal Research, Chinese Academy of Sciences, Shenyang 110016, China**
[2] *Department of Geological and Environmental Sciences, Stanford University, Stanford, California 94305, USA and*
[3] *Stanford Institute for Materials and Energy Science, SLAC National Accelerator Laboratory, Menlo Park, California 94025, USA*

We report a general scheme to systematically construct two classes of structural families of superhard sp^3 carbon allotropes of cold compressed graphite through the topological analysis of odd 5+7 or even 4+8 membered carbon rings stemmed from the stacking of zigzag and armchair chains. Our results show that the previously proposed M, bct-C_4, W and Z allotropes belong to our currently proposed families and that depending on the topological arrangement of the native carbon rings numerous other members are found that can help us understand the structural phase transformation of cold-compressed graphite and carbon nanotubes (CNTs). In particular, we predict the existence of two simple allotropes, R- and P-carbon, which match well the experimental X-ray diffraction patterns of cold-compressed graphite and CNTs, respectively, display a transparent wide-gap insulator ground state and possess a large Vickers hardness comparable to diamond.

PACS numbers: 61.50.Ks, 61.48.De, 64.60.My

Carbon exhibits numerous allotropes (fullerenes, carbon nanotubes(CNTs), graphene, graphite, diamond and amorphous carbon) thanks to its ability to form *sp*-, sp^2- and sp^3-hybridized bonds [1–3]. It is well-known that compression of graphite at high pressure (>15 GPa) and high temperature (> 1300 K)[4] leads to the formation of cubic or hexagonal diamond. In contrast, cold compression of graphite [4–15], single-walled and multi-walled CNTs [16–22] results in superhard allotropes of carbon, which were found to be intrinsically different from hexagonal (or cubic) diamond [5, 16]. Upon pressure release, the obtained cold compressed graphite phase can be quenched only at low temperature (< 100 K) [1] whereas CNT phases compressed above 75 GPa can be quenched at room temperature [16]. In addition, these high pressure phases exhibit superior mechanical performance with the ability to indent single-crystal diamond [5, 16], indicating at least comparable hardness to diamond.

However, the experimental crystal structures of these cold compressed phases of graphite and CNTs remain heavily debated. In an effort to shed light on the puzzling structural problem of cold compressed graphite several superhard sp^3-hybridized candidates (monoclinic M carbon [23, 24], body-centered tetragonal bct-C_4 carbon [25, 26], orthorhombic W [27] and Z carbon [28, 29]) have been proposed. To date, among all these proposed allotropes the most stable one is *Z* carbon [29], computationally predicted through the minima hopping method (MHM), which is exactly the same as the $oC16$-II phase proposed recently by metadynamics simulations of structural transformations [28] and the C-centered orthorhombic C_8 phase proposed by particle swarm optimization (CALYPSO) [30]. Z carbon was thought to be the best candidate [29] so far that can explain the experimental XRD peaks and Raman active mode for cold compressed graphite [5, 29]. Although Zhao *et al.* [30] argued there was a matching problem with the XRD of cold compressed graphite, they claimed [30] that the Z (namely, C_8) phase can be interpreted as the structural solution of the quenchable superhard carbon phase recovered from cold compressed CNT bundles [16]. However, we found that its XRD patterns still differ significantly compared to the experimental data (as discussed below).

If we pay more attention to the previously proposed allotropes, both W and M carbon phases can be described as corrugated graphite sheets interconnected by an alternating sequence of odd 5+7 membered rings of carbon [28]. Similarly, both bct-C_4 and Z carbon can be characterized by alternating even 4+8 membered rings. Considering all possible even and odd rings of carbon (4+8 membered rings in bct-C_4 and Z carbon, 5+7 membered rings in W and M carbon, 6-membered rings in diamond), many additional possible combinations could be expected. Therefore, it would be highly desirable to seek *a general scheme* to understand the principles of the structural formation of possible alternative superhard allotropes related to cold compressed graphite and CNTs.

In this paper, through first-principles calculations (for details, see [31]), we report on two S and B families of sp^3-hybridized superhard carbon allotropes by discussing the topological stacking of zigzag and armchair carbon chains consisting of odd 5+7 and even 4+8 membered ring patterns (see Fig. S1 [31]). Our analysis demonstrates that, after introducing the hexagonal rings which separate the periodic 5+7 or 4+8 membered patterns, a

series of new structures can be readily created. We further elucidate the energetic, mechanical and electronic properties of the obtained novel phases, confirming that all these phases are wide-gap transparent and superhard insulators. In particular, our currently proposed P carbon as well as several other new phases are energetically more favorable than the previously known most stable Z carbon [28, 30] over a large range of pressures. Moreover, we confirm that R carbon of the S-family and P carbon of the B-family are the most likely candidates so far to match the experimental data of the cold-compressed graphite [5] and CNTs [16], respectively.

Each graphite sheet (i.e., graphene) can be described as an ordered array consisting of infinite long zigzag or armchair chains of carbon atoms. The direct connection between zigzag and armchair chains results in a tilt grain boundary [32] which is interconnected by 5-membered and 7-membered rings of carbon, different form the ideal 6-membered ring in graphene. Similarly, the two-dimensional (2D) projections along the c-axis for M carbon and W carbon of cold-compressed graphite [29] are also composed of 5+7 ring patterns, realized by the repeated stacking of zigzag and armchair chains of carbon in Fig. S2 [31]. The most important feature of both M and W carbon is that each armchair chain or each zigzag chain is not infinitely long. It is recognized that carbon bonds are combined in group of four armchair or zigzag bonded chains. As illustrated in Fig. S2 [31], these four-bonds chains are interconnected by a step. Interestingly, if the directly connected zigzag and armchair chains in M carbon would be infinitely long (without any step), the simple S carbon phase could be easily realized. As shown in Fig. 1a, its 2D-projection can be described as the repeating parallel array of directly connected zigzag and armchair chains, consisting of diagonally opposed 5+7 ring pattern. If this 5+7 ring pattern is further twofold rotated, another new structure called R carbon can be formed (Fig. 1b). Therefore, the unit cell of R carbon is twice the size of S carbon.

The structures of S carbon and R carbon can be further modified. As shown in Fig. 1c and 1d, by inserting two zigzag or armchair chains to separate the 5+7 ring pattern in S carbon, two new structures (S-S_1Z_2 and S-S_1A_2) can be realized. Here, the notation of S come from the 5+7 ring patterns in S carbon (S_1 means only one S unit), whereas Z and A denote the infinitely long zigzag and armchair chains (Z_2 and A_2 refers to two zigzag and armchair chains), respectively. Furthermore, it is possible to continuously extend the number of Z and A chains to construct a series of new structures named S-S_mZ_{2n} and S-S_mA_{2n}. Here, the parameters m and n are integers (0, 1, 2 $\cdots$). Following this nomenclature, R carbon can be described as S-S_2' in which S$'$ denotes the existence of the twofold rotated symmetry of 5+7 ring pattern at variance from the normal 5+7 ring in S carbon. Following similar considerations, S$'$ can be further extended into a

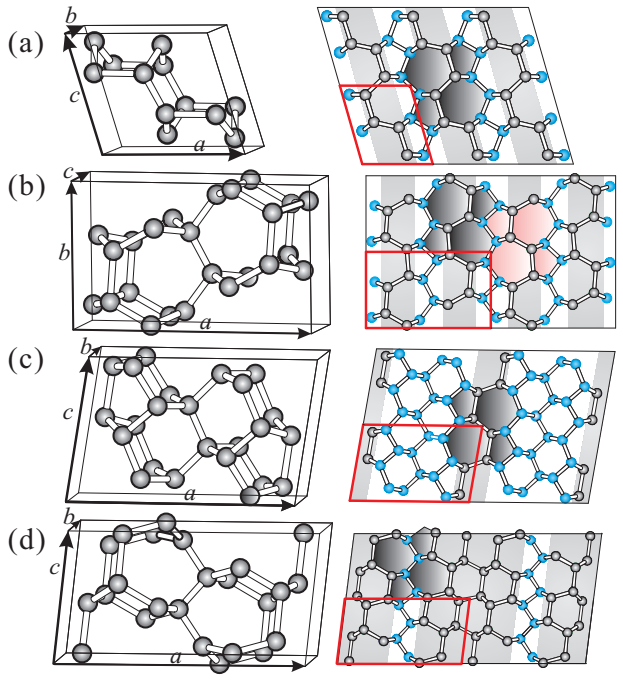

FIG. 1: (color online) (a), (b), (c) and (d) illustrate the crystallographic structures of the proposed S carbon, R carbon, S-S_1Z_2, and S-S_1A_2 phases. Left column: three-dimensional crystalline structures and right column: the two-dimensional (2D) projections of the 2×2×1 supercell along their b- or c-axis. For S carbon, the 3×1×2 supercell is used. The grey background highlights the armchair chains and white background denotes the zigzag chains.

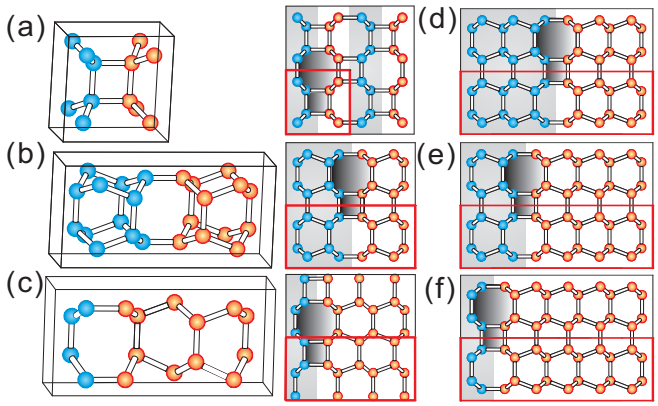

FIG. 2: (color online) (a), (b) and (c) illustrate the crystallographic structures of the bct-C_4 carbon, Z carbon, P carbon (this work). Left column: three-dimensional unit cells and right column: the 2D projections of the 2×2×1 supercell of bct-C_4 and of the 1×2×1 supercells of Z carbon along their c-axis, and the 2D projections of the 1×1×2 supercells of P carbon along its b-axis. (d), (e) and (f) show the 2D-projections in the 1×2×1 supercells along the c-axis for three typical lattice structures of the B-B_1A_4 series.

TABLE I: DFT optimized lattice constants (a, b, and c in Å) Wyckoff position(W.p.), bulk and shear moduli (B and G in GPa), estimated Vickers hardness (H_v in GPa) and theoretical density (ρ, g/cm^3) for S, R and P allotropes.

Types		W.p.	x	y	z	
S carbon	$a = 4.7302$	$2m$	0.1175	0.0	0.6746	$G = 457.7$
($P2/m$)	$b = 2.4950$	$2m$	0.5344	0.0	0.3333	$B = 412.6$
	$c = 4.0837$	$2n$	0.1131	0.5	0.8997	$H_v = 78.3$
	$\beta = 106.1°$	$2n$	0.4209	0.5	0.1319	$\rho = 3.44$
R carbon	$a = 7.7886$	$4g$	0.6731	0.9630	0.0	$G = 462.4$
($Pbam$)	$b = 4.7752$	$4g$	0.8435	0.8087	0.0	$B = 434.2$
	$c = 2.4958$	$4h$	0.9546	0.8613	0.5	$H_v = 75.0$
		$4h$	0.5704	0.8926	0.5	$\rho = 3.45$
P carbon	$a = 8.6650$	$4f$	0.5357	0.25	0.4322	$G = 485.0$
($Pmmn$)	$b = 2.4875$	$4f$	0.2077	0.25	0.4348	$B = 449.1$
	$c = 4.2160$	$4f$	0.0414	0.25	0.5625	$H_v = 78.5$
		$4f$	0.7151	0.25	0.4343	$\rho = 3.51$

series of new structures called S-S$'_m$Z$_{2n}$ and S-S$'_m$A$_{2n}$. It should be noted, that when n is increased to n+1 the number of carbon atoms in the unit cell is increased by eight atoms, due to the fact that eight carbon atoms can form a full cycle with a sixfold ring in the projections along the other b or c-axis. As such, the atom numbers of the conventional unit cells of these families are equal to $8(m + n)$.

Figure 2a shows the 2D projection of bct-C$_4$, indicating the simplest 4+8 rings pattern along the armchair orientation (direct face-to-face opposed connection of two armchair chains). By inserting the armchair chains into periodically separated 4+8 ring pattern, a new structural family of B-B$_m$A$_{2n}$ can be constructed. Here, B is the unit of the 4+8 rings composed of two opposed armchair chains originated from bct-C$_4$ and A refers to the armchair chain. For the sake of convenient comparisons, we further split A$_{2n}$ into A$_{Ln'Rn''}$ to distinguish the left- and right-armchair chain numbers of the B unit. Clearly, n'+n'' is equal to $2n$, indicating that the number of atoms is $8(m+n)$ in the conventional unit cells. With m=1 and n =0, B-B$_1$ becomes bct-C$_4$. Furthermore, the addition of two armchair chains with n=1 separates the 4+8 ring pattern thus leading to two new structures: the first one (Fig. 2b) corresponds to the Z carbon (B-B$_1$A$_{L1R1}$) as proposed in Refs. [28–30], whereas we name the second one (Fig. 2c) P carbon (B-B$_1$A$_{L0R2}$). By adding four armchair chains, n=2, three alternative structures are formed, as depicted in Fig. 2d (B-B$_1$A$_{L2R2}$), Fig. 2e (B-B$_1$A$_{L1R3}$) and Fig. 2f (B-B$_1$A$_{L0R4}$). Therefore, it is clear that all structures in the B-B$_m$A$_{2n}$ family are composed of 4+8+6 ring patterns. The introduction of zigzag chains in the 4+8 ring patterns bct-C$_4$ will lead to the occurrence of 4+8+5+7 ring complex structures. However, we do not discuss these cases since all phases associated with 4+8+5+7 ring complex (not shown here) are energetically much less stable than the S- and B-families.

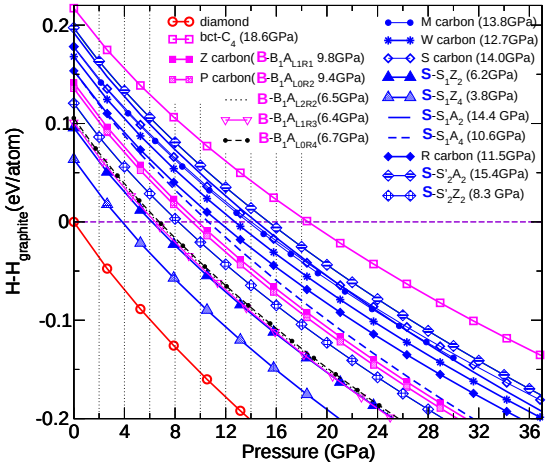

FIG. 3: (color online) Calculated enthalpy difference per atom with respect to graphite for a series of carbon allotropes as a function of pressure. The stable pressures of these proposed allotropes compared to graphite are labeled.

Figure 3 compares the relative thermodynamic stabilities of all proposed allotropes. We find that, for both S and B families with increasing zigzag or armchair units (namely, increasing the 6-membered rings in the unit cell) their structures become more stable in energy and the transition pressure associated with the structural transition decreases. This can be attributed to the introduction of more ideal 6-membered rings which actually reduces the total strain in system. If the 5+7 patterns (or 4+8 patterns) are doubly coupled in a complementary mode, the energy of system can be even lower. The complementary mode reduces the strain of system compared to the cases in which a single 5+7 (or 4+8) pattern appears in a non-coupled complementary one. Although Z and P phases share the same composition of B-B$_1$A$_2$, P carbon is more stable in energy than Z carbon (Fig. 3) because the 4+8 patterns in P carbon are always coupled doubly in a complementary mode (Fig. 2c), whereas in Z carbon they are separated by the 6-membered rings (Fig. 2b). In addition, in these families as n increases the energies of the structures approach more closely that of diamond due to the increase in the number of ideal 6-membered rings. In this situation, the S (5+7 ring) and B (4+8 ring) patterns can be thus viewed as the defect or tilt grain boundary in diamond. Following this viewpoint, the S-S$_m$Z$_{2n}$ and S-S$_m$A$_{2n}$ families can be interpreted as the combination of diamond (6-membered ring) and S carbon whereas the B-B$_m$A$_{2n}$ families show the combined character of diamond and bct-C$_4$. Furthermore, from Fig. 3 our selected phases P carbon, B-B$_1$A$_{L0R4}$, B-B$_1$A$_{L1R3}$, S-S$_1$Z$_2$, and S-S$_1$Z$_4$, are energetically more favorable than all previously theoretically proposed structures including Z carbon. In particular, even when their vibrational entropies and zero-point energies derived from phonon

densities of states are taken into account, the relative stabilities for S-, R- and P-carbon allotropes remain unchanged at least in the temperature range from 0 to 800 K at both 0 and 15 GPa.

Structural optimization revealed that R and P carbon crystallize in the orthorhombic structure whereas S carbon has a monoclinic structure (Figs. 1 and 2). The structural details of S, R, P and the other nine new allotropes proposed here are listed in Tab. 1 and Tab. S1 [31], respectively. The phonon dispersions in the whole Brillouin zone for S, R and P carbon phases have been derived, confirming their crystalline stabilities even at 0 GPa (Fig. S3 [31]). In addition, our calculations uncovered that all these allotropes exhibit large bulk and shear moduli (Table 1) which are comparable to those of diamond. Utilizing our recently proposed formula [33, 34], the Vickers hardness of S, R and P carbon are estimated to be 78.3, 75 and 78.5 GPa in Tab. 1, respectively (details refer to Tab. S3 [31]. This clearly demonstrates that these phases are superhard in agreement with the quasi-sp^3-hybrid covalent bonding framework. The HSE

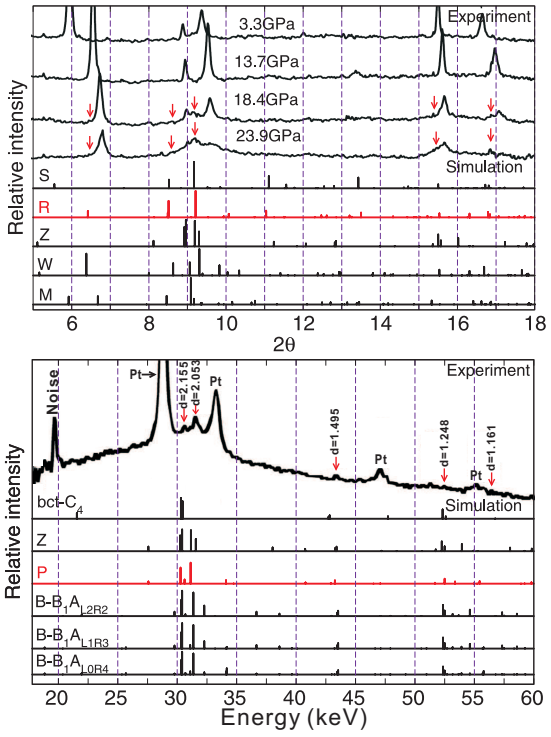

FIG. 4: (color online) (a) Simulated XRD patterns (with wavelength of 0.3329 Å) for selected phases at 18.4 GPa compared with experimental results from Ref. [5] for cold-compressed graphite. (b) Simulated XRD patterns of the five allotropes in B family at ambient pressure, in comparison with the date measured from the quenchable phase recovered from cold-compressed CNTs [16]. The red arrows highlight five main experimental peaks.

electronic band structures illustrate that S-, R-, and P-carbon are all wide-gap transparent insulators with band gaps ranging between 3.9 and 5.5 eV (Fig. S3 [31]). In particular, both S and R carbon have the widest direct band gap at Γ (about 5.5 eV) among all known allotropes discussed here.

Although Z carbon was identified as a good candidate of cold compressed graphite in the latest work [29], this was challenged by Zhao *et al.* [30] due to the problems for matching experimental XRD patterns. They demonstrated that its simulated patterns match neither the experimental peak at 16.8° and nor the gradually decreased peak density around 9.0° [30] for cold-compressed graphite (for details, see the online supporting materials of Ref. [29]). Importantly, we found that the simulated XRD patterns of R carbon match much better the experimental data for five main peaks as marked by arrows in Fig. 4(upper panel). The obtained pressure of 11.5 GPa for the stability of R carbon is consistent with the experimental value. Therefore, R carbon can be considered as a highly likely candidate for cold-compressed graphite.

Furthermore, we found that P carbon is a better candidate to interpret the experimental XRD pattern of cold-compressed CNTs than Z carbon as claimed in Ref. [30]. From Fig. 4 (lower panel), for Z carbon and three other B-family phases (B-B_1A_{L2R2}, B-B_1A_{L1R3}, B-B_1A_{L0R4}) the simulated peaks at d = 2.155 Å are stronger (or at least comparable) than the ones at 2.053 Å. This notion is not consistent with the reported XRD patterns [16] which clearly revealed the d=2.053 Å peak has the highest intensity. This fact suggests that Z carbon may not be a good candidate of cold-compressed CNTs. Nevertheless, it is exciting to note that the simulated XRD pattern of P carbon shows a significantly improved agreement with the experimental data. Its five main peaks at d = 2.167 Å, 2.107 Å, 1.510 Å, 1.244 Å and 1.179 Å give satisfactory accordance in both locations and intensities with experimental d spacings of 2.155 Å, 2.053 Å, 1.495 Å, 1.248 Å and 1.161 Å respectively (see Fig. 4(lower panel)). Besides, its theoretical bulk density (ρ= 3.51 g/cm^3) and bulk modulus (B = 449.1 GPa) are in nice agreement with the experimental data (ρ = 3.6±0.2 g/cm^3 and B = 447 GPa), see Tab. 1 and S2 [31].

In summary, R-carbon in the S-family and P-carbon in the B-family have been found to best match with the experimental data of cold-compressed graphite and CNTs, respectively. Moreover, for all other proposed allotropes related to the S- and B-families, the simulated XRD patterns also capture their main experimental features. In general, with increasing numbers of zigzag or armchair units, the main peaks remain essentially unchanged (see Fig. S4 [31]), though their corresponding 2θ values are slightly shifted. Considering that in real samples a pressure gradient could exist [5, 16] and the tube diameters of CNTs show a wide range from 1.8 to 5.1 nm [16] which may create the conditions of the formation of different

phases [25, 35], it would be reasonable to expect that the cold-compressed phase of graphite and CNTs can be interpreted as a mixture of several of the proposed allotropes.

Acknowledgements: We gratefully acknowledge fruitful discussions with Z. Z. Zhang, K.-M. Ho, and C. Franchini. This work was supported by the "Hundred Talents Project" of Chinese Academy of Sciences and from NSFC of China (Grand Number: 51074151) as well as Beijing Supercomputing Center of CAS (including its Shenyang branch). W.L.M. and S.W. were supported by EFree, an Energy Frontier Research Center funded by the U.S. Department of Energy, Office of Science, Office of Basic Energy Sciences under Award Number DE-SG0001057.

* Corresponding author: xingqiu.chen@imr.ac.cn

[1] E. D. Miller, D. C. Nesting and J. V. Badding, Chem. Mater., **9**, 18 (1997).
[2] A. Hirsch, Nat. Mater., **9**, 868 (2010).
[3] P. Ehrenfreund and B. H. Foing, Science, **329**, 1159 (2010).
[4] F. P. Bundy, W. A. Bassett, M. S. Weathers, R. J. Hemley, H. K. Mao and A. F. Goncharov, Carbon, **34**, 141-153 (1996).
[5] W. L. Mao, H-K. Mao P. J. Eng, T. P. Trainor, M. Newville, C-C. Kao, D. L. Heinz, J. F. Shu, Y. Meng and R. J. Hemley, Science, **302**, 425 (2003).
[6] R. B. Aust and H. G. Drickamer, Science, **140**, 817 (1963).
[7] F. P. Bundy and J. S. Kasper, J. Chem. Phys., **46**, 2437 (1967).
[8] A. F. Goncharov, I. N. Makarenko and S. M. Stishov, Sov. Phys. JETP, **69**, 380 (1989).
[9] A. F. Goncharov, Zh. Eksp. Theo. Fiz., **98**, 1824 (1990).
[10] M. Hanfland, H. Beister and K. Syassen, Phys. Rev. B, **39**, 12598 (1989).
[11] Y. X. Zhao and I. L. Spain, Phys. Rev. B, **40**, 993 (1989).
[12] W. Utsumi and T. Yagi, Science, **252**, 1542 (1991).
[13] M. Hanfland, J. Z. Hu, J. F. Shu, R. J. Hemley, H. K. Mao and Y. Wu, Bull. Amer. Phys. Soc., **35**, 465 (1990).
[14] T. Yagi, W. Utsumi, M. Yamakata, T. Kikegawa and O. Shimomura, Phys. Rev. B, **46**, 6031 (1992).
[15] J. M. Montgomery, B. Kiefer and K. K. M. Lee, J. Appl. Phys., **110**, 043725 (2011).
[16] Z. W. Wang, Y. S. Zhao, K. Tait, X. Z. Liao, D. Schiferl, C. S. Zha, R. T. Downs, J. Qian, Y. T. Zhu and T. D. Shen, PNAS, **101**, 13699 (2004).
[17] J. Tang, L.-C. Qin, T. Sasaki, M. Yudasaka, A. Matsushita and S. Iijima, Phys. Rev. Lett., **85**, 1887 (2000).
[18] V. N. Khabashesku, Z. N. Gu, B. Brinson, J. L. Zimmerman and J. L. Margrave, J. Phys. Chem. B, **106**, 11155 (2002).
[19] M. Popov, M. Kyotani, R. J. Nemanich and Y. Koga, Phys. Rev. B, **65**, 033408 (2002).
[20] M. Popov, M. Kyotani and Y. Koga, Diamond and Related Materials, **12**, 833 (2003).
[21] M. J. Bucknum and E. A. Castro, J. Chem. Theory Comput., **2**, 775 (2006).
[22] R. S. Kumar, M. G. Pravica, A. L. Cornelius, M. F. Nicol, M. Y. Hu and P. C. Chow, Diamond & Related Materials, **16**, 1250 (2007).
[23] Q. Li, Y. M. Ma, A. R. Oganov, H. B. Wang, H. Wang, Y. Xu, T. Cui, H-K. Mao and G. T. Zhou, Phy. Rev. Lett., **102**, 175506 (2009).
[24] A. R. Oganov, C. W. Glass, The Journal of chemical physics, **124**, 244704 (2006).
[25] Y. Omata, Y. Yamagami, K. Tadano, T. Miyake, and S. Saito, Physica E **29**, 454 (2005).
[26] K. Umemoto, R. M. Wentzcovitch, S. Saito and T. Miyake, Phy. Rev. Lett., **104**, 125504 (2010).
[27] J.-T. Wang, C. F. Chen and Y. Kawazoe, Phy. Rev. Lett., **106**, 075501 (2011).
[28] D. Selli, I. A. Baburin, R. Martonnak and S. Leoni, Phys. Rev. B, **84**, 161411R (2011).
[29] M. Amsler, J. A. Flores-Livas, L. Lehtovaara, F. Balima, S. Alireza, et al., arXiv: 1109.1158 (2011). Phys. Rev. Lett., (accepted).
[30] Z. S. Zhao, B. Xu, X. F. Zhou, L.-M. Wang, B. Wen, J. L. He, Z. Y. Liu, H.-T. Wang and Y. J. Tian, Phys. Rev. Lett., **107**, 215502 (2011).
[31] See supplementary material at http://link.aps.orgsupplementary/.
[32] R. Granta, V. B. Shenoy and R. S. Ruoff, Science, **330**, 946 (2011).
[33] X.-Q. Chen, H. Y. Niu, D. Z. Li and Y. Y. Li, Intermetallics, **19**, 1275 (2011).
[34] X.-Q. Chen, H. Y. Niu, C. Franchini, D. Z. Li and Y. Y. Li, Phys. Rev. B, **84**, 121405(R) (2011).
[35] M. Sakurai and S. Saito, Physica E **43**, 673 (2011).